Potentials for modeling cold collisions between Na (3S) and Rb (5S) atoms

A. Pashov
Department of Physics, Sofia University, 5 James Bourchier Boulevard, 1164 Sofia, Bulgaria

O. Docenko, M. Tamanis, and R. Ferber
Department of Physics and Institute of Atomic Physics and Spectroscopy, University of Latvia, 19 Rainis Boulevard, Riga LV-1586, Latvia

H. Knöckel and E. Tiemann
Institut für Quantenoptik, Universität Hannover, Welfengarten 1, 30167 Hannover, Germany
(Received 4 October 2005; published 21 December 2005)

The experimental characterization of the electronic states correlated to the asymptote of ground state Na (3S) and Rb (5S) atoms was expanded by spectroscopic data on $a\,^3\Sigma^+$ state levels using a high resolution Fourier transform spectroscopy technique. The hyperfine splitting of the $a\,^3\Sigma^+$ state levels was partially resolved and analyzed for both Na ^{85}Rb and Na ^{87}Rb isotopomers. Transitions to high lying levels of the $a\,^3\Sigma^+$ and $X\,^1\Sigma^+$ states were recorded simultaneously which enables one to determine long range parameters of the molecular potentials. Coupled channels calculations based on the Fourier grid method were finally applied for deriving accurate potential energy curves of the $a\,^3\Sigma^+$ and $X\,^1\Sigma^+$ states capable of a reliable description of cold collisions between Na and Rb atoms in their ground states. Scattering lengths and Feshbach resonances were calculated for some quantum states.

DOI: 10.1103/PhysRevA.72.062505 PACS number(s): 31.50.Bc, 33.20.Kf, 33.20.Vq, 33.50.Dq

I. INTRODUCTION

The pair of Na and Rb atoms is presently one of the interesting objects in experiments with mixed alkali-metal species at ultracold temperatures. Photoassociation, ultracold collision, and trap loss experiments were reported for a large number of such mixed species like Na-Li [1], Na-Rb [2], Na-Cs [3,4], K-Rb [5–7], Rb-Cs [8], etc. It was observed that heteronuclear trap losses present characteristic dependence on light intensity and a variety of inelastic collision processes will play a role. Therefore, reliable potential energy curves for modeling and understanding cold collision phenomena are needed.

Some electronic states of the NaRb molecule have been studied experimentally (see e.g., Refs. [9–14] and references therein), but efforts are still needed in order to refine and also to extend the experimental potentials to long internuclear distances which would allow a consistent picture of experiments like photoassociation. On the long range part accurate theoretical calculations exist [15–17] and extending with them the experimentally determined potentials first calculations on scattering properties for Na-Rb were reported [18–21].

The present contribution is devoted to the asymptote of a ground state pair of Na and Rb atoms, which has been studied experimentally in Refs. [11,22], however, only energy levels of the $X\,^1\Sigma^+$ molecular state [see Fig. 1(a)] were covered. The highest observed rovibrational level had $v_X=76$ which lies about 4.5 cm^{-1} below the asymptote. In order to derive more reliable potentials at large internuclear distances it is necessary to collect experimental data closer to the asymptote and to include transitions to energy levels of the lowest triplet state $a\,^3\Sigma^+$ which correlates also to the pair of ground state Na and Rb atoms and for which until now the experimental data were scarce [9] or obtained at low resolution [23]. Constructing the appropriate Hamiltonian for the problem, it should be taken into account that both states, a and X, couple by hyperfine interaction, which for the most weakly bound states is of the same order of magnitude as the binding energy itself. Thus close to the asymptote these states loose their triplet or singlet character and coupled channels treatment should be applied.

In this paper we report on two experimental approaches which allowed us to come closer to the Na(3S)+Rb(5S) asymptote and to measure data for both the singlet and the triplet molecular electronic states. The hyperfine splitting of the $a\,^3\Sigma^+$ state levels was analyzed and the atomic constants of the Fermi contact interaction were found adequate to explain the structure of all observed experimental levels within the obtained resolution. Accurate potential energy curves extending to the region of long internuclear distances were determined in a coupled channels treatment. The experimental long range potentials confirm the good quality of the theoretical dispersive coefficients [15–17]. The derived potentials are applied for calculations of scattering lengths and Feshbach resonances both for Na-^{85}Rb and for Na-^{87}Rb pairs.

II. EXPERIMENT

The electronic structure of the NaRb molecule was studied by means of high resolution Fourier transform spectroscopy. Details on the experimental setup can be found in Ref. [11] and will be mentioned only briefly here. The molecules were prepared in a stainless steel heat pipe oven by heating a mixture of metallic Na and Rb up to 600 K. Visible and near infrared molecular fluorescence induced by a variety of laser sources was resolved by a Bruker IFS 120 HR Fourier trans-

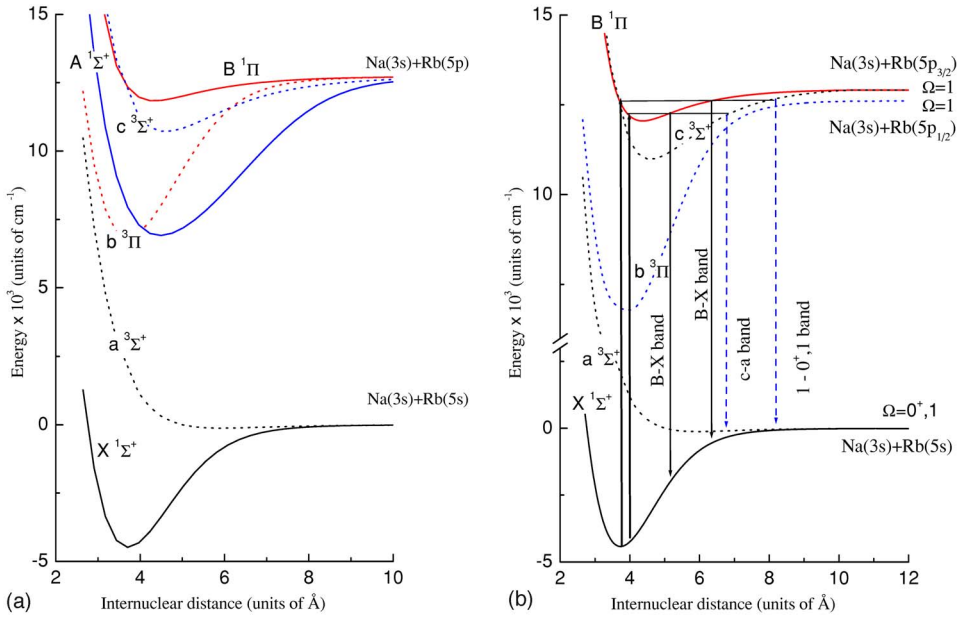

FIG. 1. (Color online) (a) Theoretical potentials for NaRb [24]. (b) Excitation schemes for studying the electronic states correlating to the Na(3S)+Rb(5S) asymptote. For clarity the fluorescence bands are indicated only by the corresponding triplet or singlet component of the $B\,^1\Pi$-$b\,^3\Pi$-$c\,^3\Sigma^+$ complex.

form spectrometer with a typical resolution of 0.01 cm^{-1}–0.03 cm^{-1}.

As has been already mentioned the goal of these experiments is twofold; collecting data close to the molecular ground state asymptote and extending the experimental information to the triplet $a\,^3\Sigma^+$ state, see Fig. 1(a). A well known technique for reaching the triplet manifold from singlet states is through singlet and triplet molecular states mixed by perturbations (e.g., the spin-orbit coupling). Such perturbations between the $B\,^1\Pi$, $b\,^3\Pi$, and $c\,^3\Sigma^+$ states were reported by Wang *et al.* [23,24]. Therefore, we used a Rhodamine 6 G single mode dye laser (Coherent 699-21) and excited transitions to levels of the $B\,^1\Pi$, $b\,^3\Pi$, and $c\,^3\Sigma^+$ complex, see Fig. 1(b). In Fig. 2(a) we present a typical fluorescence spectrum, where along with the $B \rightarrow X$ band system, a weaker band appears around 12 100 cm^{-1}, which is due to decay to the $a\,^3\Sigma^+$ state, together with a continuum spectrum from bound-free emission to the repulsive branch of the $a\,^3\Sigma^+$ state. This type of progression to the triplet state originates from the mixture of relatively low vibrational levels of the B state with levels of the triplet b and c states.

In order to observe transitions to weakly bound singlet and triplet ground state levels from a common upper level we took advantage of the long range changeover of the coupling case, namely that close to the atomic asymptote the Hund's case (a) and (b) electronic states develop to the Hund's case (c) coupling and finally to the Hund's case (e) where the electronic angular momenta are uncoupled from the molecular axis. That is, the main perturber of the $B\,^1\Pi$ state, the c state, at long internuclear distances becomes a mixed state with triplet and singlet character giving rise to transitions to the ground a and X states. These transitions between case (c) states are indicated by dashed vertical arrows in Fig. 1(b).

In our experiments we observed several spectra which we interpret by such long range changeover. In Fig. 2(b) an example of the resolved fluorescence is shown when exciting a high vibrational B state level ($v'_B=25$) mixed with c state levels. Similar to Fig. 2(a) bands to the X and a states are seen. In the same figure the calculated Franck-Condon factors (FCF) for B-X transitions are shown as crosses. The FCFs were calculated applying a B state potential based on the molecular constants from Ref. [24] and new measurements with polarization labeling spectroscopy [25]. The FCFs give reasonable agreement with the experimental intensities down to approximately 12 700 cm^{-1}, where the FCFs predict the end of the B-X band. In reality we observed a continuation of this fluorescence progression down to 12 500 cm^{-1} where it appears simultaneously with the corresponding transitions to the a state from the common upper state level. These additional transitions to the X state are due to the long range changeover of the c state to Hund's case (c).

A typical portion of the spectrum containing Q type ($\Delta J=0$) transitions with $J'=19$ is shown in Fig. 3 reaching $v_a=18$ of the $a\,^3\Sigma^+$ state and $v_X=78$ of the $X\,^1\Sigma^+$. The assignment of the triplet state levels is according to the vibrational numbering established in this study below. Similar spectra were recorded for a wide range of J' quantum numbers ($J'=10-23$) including also P- and R-type ($\Delta J=\pm 1$) transitions. In this way abundant information on the near asymptotic levels of the $a\,^3\Sigma^+$ and $X\,^1\Sigma^+$ states was collected. These spectra are particularly interesting also because they show directly the whole pattern of singlet and triplet levels for a given rotational quantum number close to the asymptote, so it should be possible to establish the coupling between the $a\,^3\Sigma^+$ and the $X\,^1\Sigma^+$ state levels through hyperfine interaction and to distinguish the exchange energy.

It is worth mentioning that when exciting above the ($3S+5P_{1/2}$) asymptote no such progressions were observed, probably due to predissociation of the $\Omega=1$ ($3S+5P_{3/2}$) levels caused by coupling to the continuum above the asymptote ($3S+5P_{1/2}$).

The total data set for the $a\,^3\Sigma^+$ state consists of more than 900 transition frequencies to 491 energy levels as shown in Fig. 4 for both isotopomers $^{23}Na\,^{85}Rb$ and $^{23}Na\,^{87}Rb$. The

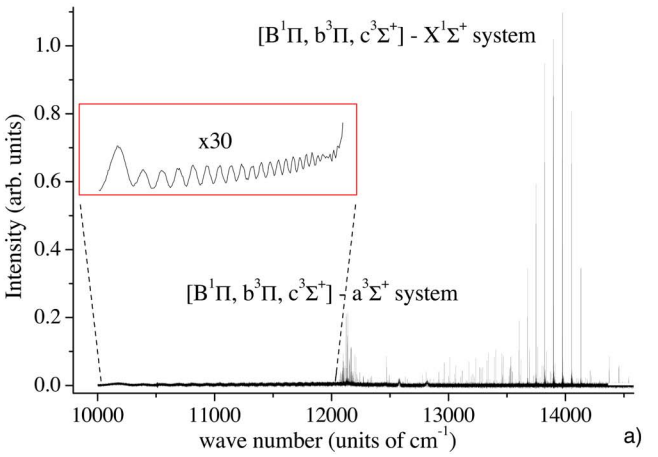

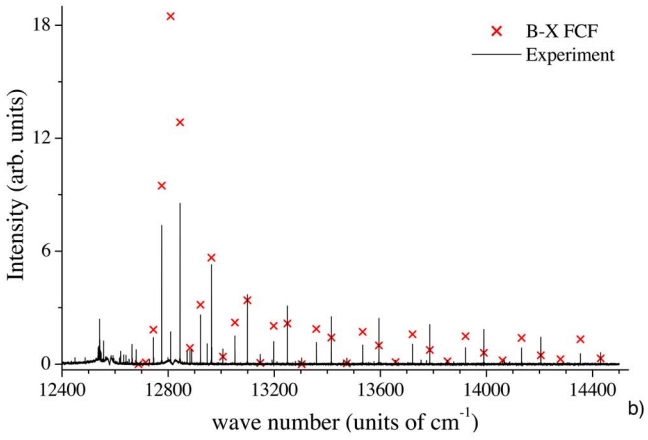

FIG. 2. (Color online) (a) Fluorescence progressions to the $a\ ^3\Sigma^+$ and $X\ ^1\Sigma^+$ state levels from levels of the complex of the coupled $B\ ^1\Pi$-$b\ ^3\Pi$-$c\ ^3\Sigma^+$ electronic states excited by a Rhodamine 6 G dye laser at 16 927.97 cm^{-1}. (b) A comparison between the calculated Franck-Condon factors (FCF) for the B-X transitions (crosses) and the experimental intensities of the fluorescence progression excited at 17 377.37 cm^{-1}. The absorption of the molecular fluorescense by the atomic Rb D2 line is the reason for low line intensities around 12 800 cm^{-1} compared to prediction by FCF. The band seen below 12 600 cm^{-1} is an overlap of singlet and triplet structure.

experimental uncertainty was estimated to be 0.003 cm^{-1} for lines recorded with good signal-to-noise ratio (SNR$>$5). The data set for the $X\ ^1\Sigma^+$ state published in Ref. [11] was correspondingly enriched by about 250 transitions adding some 150 new rovibrational levels (The full lists of experimental frequencies to the $a\ ^3\Sigma^+$ state and the new transitions to the $X\ ^1\Sigma^+$ state are given as a supplement (see Ref. [39]).

III. MODELING THE EXPERIMENTAL OBSERVATIONS

The adequate model for description of the above mentioned experimental observations differs from the single potential approach used in Ref. [11]. Close to the molecular asymptote the $X\ ^1\Sigma^+$ and the $a\ ^3\Sigma^+$ states are coupled by the

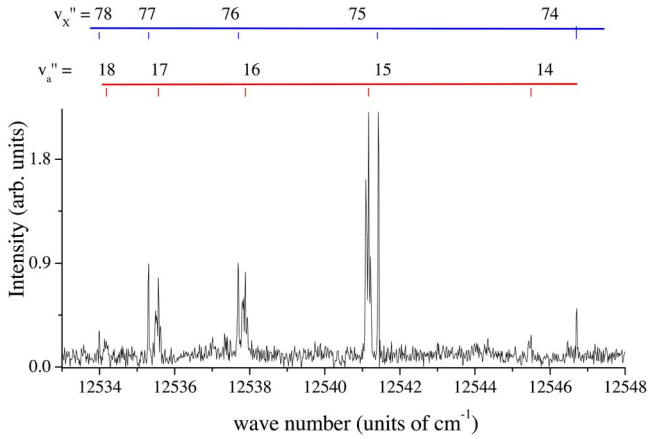

FIG. 3. (Color online) Transitions to levels near the Na(3S)+Rb(5S) asymptote for $J''=N''=19$ of Na ^{85}Rb [30]. The assignment of the triplet state levels is according to the vibrational numbering established in this study.

hyperfine interactions and coupled channels calculations should be applied (see, e.g., Refs. [26,27]). Far from the asymptote the levels of the $a\ ^3\Sigma^+$ state are split by the Fermi contact interaction (see a detailed discussion in Ref. [9]) which was resolved in our experiment as well. Therefore, we first analyzed the hyperfine structure of the triplet ground state in order to determine to which extent it is influenced by the vibration and rotation of the molecule. Then the hyperfine structure was subtracted from the observations and such constructed levels sufficiently below the atomic asymptote were incorporated in a single potential fit for the $a\ ^3\Sigma^+$ state as done for example for I_2 in Ref. [28]. Finally, the long range parts of the $X\ ^1\Sigma^+$ and the $a\ ^3\Sigma^+$ states potentials were adjusted in iterative coupled channel calculations in order to take into account simultaneously all interactions which contribute to the energy structure of both states $X\ ^1\Sigma^+$ and $a\ ^3\Sigma^+$ near the asymptote as observed in the present experiments.

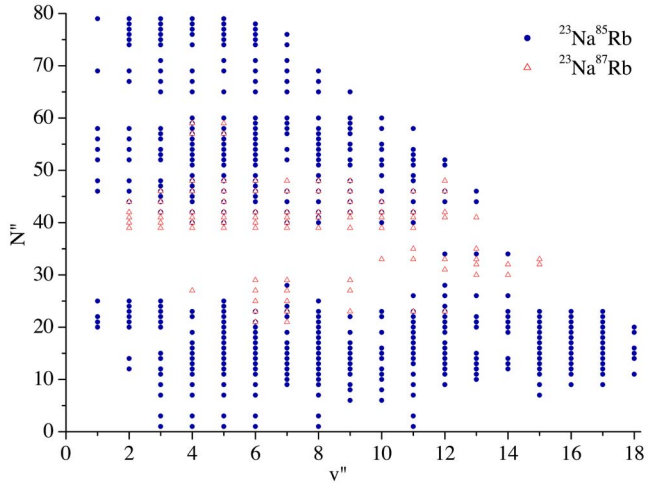

FIG. 4. (Color online) The range of vibrational and rotational quantum numbers of the observed energy levels in Na ^{85}Rb and Na ^{87}Rb.

A. Analysis of the hyperfine splitting of the $a\ ^3\Sigma^+$ state levels

The hyperfine splitting of the $a\ ^3\Sigma^+$ levels is caused by the Fermi contact interaction and the appropriate theory was described in detail by Kasahara *et al.* [9] for Na ^{85}Rb in low vibrational levels of the $a\ ^3\Sigma^+$ state. The effective Hamiltonian for the electronic spin S and the nuclear spin I defines the interaction parameters:

$$H = A_{\mathrm{Rb}} \cdot S_{\mathrm{Rb}} \cdot I_{\mathrm{Rb}} + A_{\mathrm{Na}} \cdot S_{\mathrm{Na}} \cdot I_{\mathrm{Na}}. \quad (1)$$

From the experimental spectra the A_{Na} and A_{Rb}^{85} constants were determined which describe the observed splitting within a Hund's case $b_{\beta S}$ coupling scheme. Generally, the molecular coupling parameters correspond to the atomic constants A. But for atoms forming a diatomic molecule the dependence of these parameters on the bond length and thus on the vibrational and rotational quantum numbers cannot be excluded (see Ref. [28]). Within the resolution of our experiment we recorded a partially resolved hyperfine structure of the $a\ ^3\Sigma^+$ state levels and since our data covered a much broader range of $a\ ^3\Sigma^+$ levels of both isotopomers than in Ref. [9] we checked the dependence of A_{Na}, A_{Rb}^{85}, and A_{Rb}^{87} on the vibrational and rotational quantum numbers and determined the A_{Rb}^{87} constant for Na ^{87}Rb.

In Fig. 5 examples of the observed hyperfine splittings of transitions to $a\ ^3\Sigma^+$ state levels in Na ^{85}Rb and Na ^{87}Rb are shown. Within the resolution of the present experiment these splittings are the same in each isotopomer group for almost all observed rovibrational levels of the $a\ ^3\Sigma^+$ state. The only feature, where slight deviations from the pattern in Fig. 5 were observed, is for $v_a=16$ in Na ^{85}Rb. These deviations, however, are most likely due to the local perturbation by the $v_X=76$ level of the $X\ ^1\Sigma^+$ state separated by only several tenths of a wave number and this interpretation is confirmed in Sec. III C. Therefore, extending the range of observations from Ref. [9], we found that the hyperfine splitting of the $a\ ^3\Sigma^+$ state for both isotopomers is characterized by two constants which are very close to those of the corresponding free atoms. A comparison for A_{Rb}^{85} and A_{Na}^{23} was done in Ref. [9]. Our value for $A_{\mathrm{Rb}}^{87}=0.113(1)$ cm^{-1} also agrees with the atomic parameter 0.11 399 cm^{-1} [30].

The hyperfine structure (HFS) free positions of the triplet state levels are shifted from the central component of the hyperfine pattern (see Fig. 5) by 0.017 cm^{-1} for Na ^{85}Rb and by 0.062 cm^{-1} for Na ^{87}Rb. By using these energy levels potentials without HFS, corrections will be obtained.

B. Single potential fit for $a\ ^3\Sigma^+$

The levels corrected for hyperfine structure were used to construct a potential curve for the $a\ ^3\Sigma^+$ state in a manner similar to that used for the $X\ ^1\Sigma^+$ state [11]. Briefly, for short and intermediate internuclear distances the potential curve is represented by a set of points connected with natural cubic spline functions [31]. In order to reduce any undesired oscillations of the curve close to the asymptote caused by a too high flexibility of the spline representation we applied the regularization technique reported in Ref. [32]. Initially, the potential was adjusted to fit all constructed 1935 differences

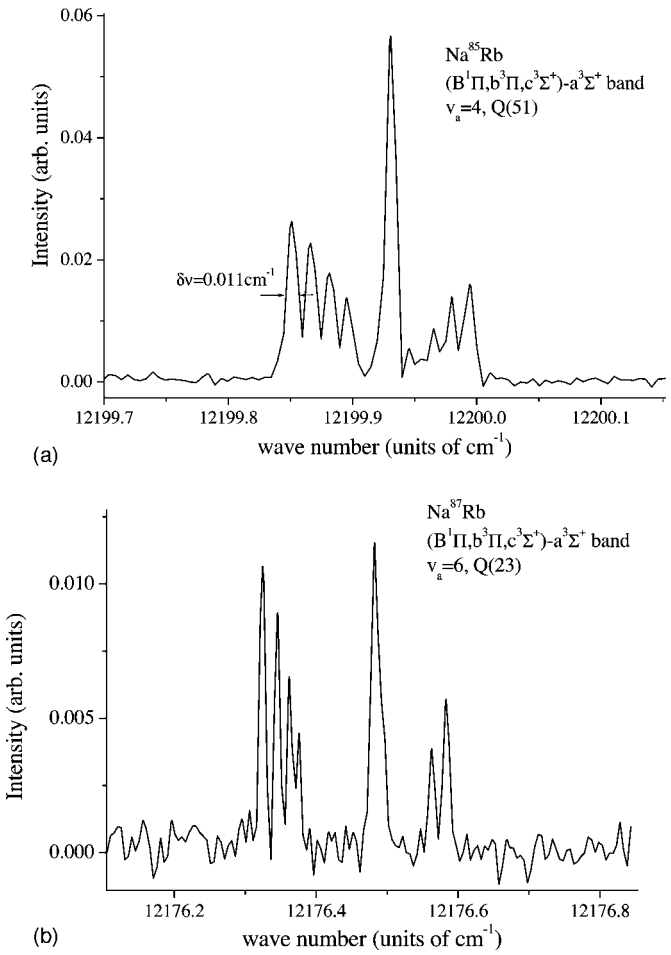

FIG. 5. Hyperfine splitting of the transitions to the $a\ ^3\Sigma^+$ state in Na ^{85}Rb and Na ^{87}Rb.

between the observed line positions in both isotopomers. Once relatively good agreement between calculated and measured differences was achieved we excluded from the fit high vibrational levels since we expected possible shifts due to interactions with the $X\ ^1\Sigma^+$ state.

As an approximate potential for the fit we adopted the curve from Ref. [33]. Unfortunately, all our attempts to reach quantitative agreement with the experimental observations failed and we obtained systematic deviations up to 0.05 cm^{-1}. The same happened when trying to fit data only for one of the isotopomers. After we analyzed possibilities for additional second order spin-spin and spin-rotation interactions we concluded that their magnitude should be much smaller than our experimental uncertainty and therefore, they cannot explain the deviations. Then we decided to revise the vibrational numbering of the $a\ ^3\Sigma^+$ state established for the first time in Ref. [23] and afterwards used in Ref. [33]. In fact, our observed spectra do not show any vibrational level below the level named $v_a=0$ in Ref. [23]. However, when we shifted the vibrational numbering by one vibrational quantum, i.e., now the lowest observed levels became $v_a=1$, we achieved almost immediately a good fit for $v_a<15$ in Na ^{85}Rb and the same potential was able to describe the experimental observations in Na ^{87}Rb within their uncertainty without additional adjustment. The high quality of the fit

including low vibrational levels ($v_a=1$) from both isotopomers with a single potential curve is taken as a proof for the correctness of this assignment. Additionally, we also tried fits by shifting the vibrational numbering by two and three quanta which were not successful.

C. Analysis by coupled channels calculations

The final forms of the $a\,^3\Sigma^+$ and $X\,^1\Sigma^+$ state potentials were determined in a coupled channels analysis which takes into account the hyperfine interaction between these states.

The absolute position of the $a\,^3\Sigma^+$ state in the energy scale with respect to the $X\,^1\Sigma^+$ state was adjusted so that the spacings between eigenenergies of both potentials agree with the separation of spectral lines decaying to the corresponding energy levels from a common upper state level (see, e.g., Fig. 3). Here the hyperfine splitting of the triplet state levels was taken into account. This procedure was performed for levels far from the asymptote to avoid possible shifts due to the hyperfine interaction.

For large internuclear distances (typically larger than 11 Å) we adopted the standard long range form of molecular potentials

$$U_{\mathrm{LR}}(R) = U_\infty - C_6/R^6 - C_8/R^8 - C_{10}/R^{10} \pm E_{\mathrm{exch}}, \qquad (2)$$

where the exchange contribution is given by

$$E_{\mathrm{exch}} = A_{\mathrm{ex}} R^\gamma \exp(-\beta R). \qquad (3)$$

U_∞ is the energy of the atomic asymptote (excluding the hyperfine energies) with respect to the minimum of the $X\,^1\Sigma^+$ state. It coincides with the dissociation energy of this state, D_e^X. The exchange energy is repulsive for the triplet state [plus sign in (2)] and attractive for the singlet state (minus sign). All parameters in Eqs. (2) and (3) are common for the $X\,^1\Sigma^+$ and $a\,^3\Sigma^+$ states.

As a first guess we used the already published long range parameters for the $X\,^1\Sigma^+$ state [11] also for the triplet $a\,^3\Sigma^+$ state. For the exchange energy we adopted the estimation done in Ref. [18]. The connecting points between the short and the long range potentials were chosen such that a continuous and smooth transition between the two representations for R below or above the connection point R_o is ensured.

Since the analysis of the molecular hyperfine structure has shown that the corresponding splitting is independent of the vibrational and rotational structure and on average agrees with the atomic values, the interactions that couple the $a\,^3\Sigma^+$–$X\,^1\Sigma^+$ system can be modeled by the atomic hyperfine splitting of the corresponding atoms. The total Hamiltonian describing the interactions between ground state Na and Rb atoms is similar to that given in Ref. [34] and is adapted for the case of different atomic species. Details on such calculations have been discussed in Ref. [35] for the case of Na_2. Our coupled channels code is based on the Fourier grid Hamiltonian method.

Preliminary coupled channels calculations with potential curves determined in single channel fits showed that the shifts of the calculated energy levels with respect to the unperturbed ones, i.e., the eigenvalues of the single potentials, exceed the experimental uncertainty only for $v_X \geqslant 74$ of the $X\,^1\Sigma^+$ state and $v_a \geqslant 14$ of the $a\,^3\Sigma^+$ state. The strongest one is the coupling between the $v_X=76$ of the $X\,^1\Sigma^+$ state and $v_a=16$ of the $a\,^3\Sigma^+$ state in agreement with our experimental observations on the hyperfine structure. For these levels the coupling leads to shifts of the order of 0.02 cm^{-1}. Generally, however, although shifted, the whole pattern of the hyperfine splitting is preserved so that the levels can still be classified as singlet and triplet in the studied region. This is further confirmed by calculating the expectation values of the magnitude of the total spin operator $\boldsymbol{S}$ for levels within the coupled system; these differ by no more than few percent from 0 or 1 for the observed levels but must be altered for levels closer to the asymptote. As a next step of analysis the molecular potentials for the singlet and triplet ground states were fitted by taking into account the coupling between them. The coupled channels calculations are quite time consuming due to the large number of observed rotational quantum numbers, and it would be inefficient to fit the potentials directly as a coupled system. The following iterative procedure was adopted instead; first the shifts of the calculated levels of the coupled system with respect to the eigenenergies of single potentials were determined as a first order correction, because the initial potentials were already a good approximation. Therefore, the experimental data were corrected by the corresponding shifts and molecular potentials were fitted to the corrected experimental data in a single channel fit. Thus a better approximation of the potentials was obtained and the procedure was repeated until the experimental data were described by the coupled channels calculations within the experimental uncertainties.

In the single channel fit only the dissociation energy, the dispersion coefficients, and the exchange energy parameter A_{ex} were adjusted assuming the long range expression (2) to be valid beyond R_o, approximately 11 Å. These parameters were fitted simultaneously to the experimental data for the $X\,^1\Sigma^+$ and the $a\,^3\Sigma^+$ states. When a change of the long range parameters led to discontinuity in the connecting point R_o, the connecting point was shifted and/or separate fits of the pointwise representations of the potentials were carried out.

In several iterations we obtained the potentials listed in Tables I and II. For convenience quantities like T_e (position of the potential minimum), R_e (equilibrium distance), and D_0 (dissociation energy with respect to the first rovibrational level $v''=0$, $J''=0$) are given. In order to assess the quality of the fitted potentials a combined data set was constructed, in addition to the experimental data sets sorted separately for transitions to the singlet and the triplet state. It contains all transitions to high vibrational levels of both states ($v_X>74$ and $v_a>14$). Differences between these selected transition frequencies were calculated not only between the transitions to a given electronic state, as done before, but also differences between transitions to different states were formed. This is possible since by a single excitation transitions to both the singlet and the triplet state were observed. Extremely precious are progressions appearing by the so called long range changeover, since they contain information about high vibrational levels of both states and allow the separation between the states near the asymptote to be precisely estimated. The combined data set contains 555 transition fre-

TABLE I. Pointwise representation of the potential energy curve for the $X\ ^1\Sigma^+$ state of NaRb.

R [Å]	U [cm^{-1}]	R [Å]	U [cm^{-1}]
2.100000	23623.67465	5.791989	3880.39592
2.200000	17634.41477	5.973808	4088.60966
2.300000	13279.18859	6.155626	4262.33458
2.400000	10069.56048	6.337444	4405.67319
2.500000	7667.49769	6.519263	4522.91885
2.600000	5874.22172	6.701081	4618.17079
2.700000	4521.74692	6.882899	4695.19866
2.800000	3427.90598	7.064718	4757.28897
2.900000	2528.63531	7.246536	4807.26121
3.000000	1798.65045	7.428355	4847.46365
3.131998	1060.60559	7.610173	4879.81088
3.263996	544.13656	7.791991	4905.89082
3.395993	215.36397	7.973810	4926.95998
3.527991	43.57832	8.155628	4944.02973
3.659989	0.83395	8.499301	4968.08811
3.791987	62.11989	8.699301	4978.43703
3.973805	276.44925	8.899301	4986.78123
4.155624	597.14349	9.192121	4996.27537
4.337442	984.16758	9.514223	5003.97364
4.519260	1405.59678	9.942941	5011.19667
4.701079	1836.47101	10.461689	5016.98016
4.882897	2257.79571	11.152144	5021.73265
5.064716	2655.74803	12.101429	5025.42308
5.246534	3020.92992	13.050715	5027.33721
5.428352	3347.84205	14.000000	5028.47884
5.610171	3634.22011		
U_∞=5030.50235 cm^{-1}			
R_o=11.2967 Å			
C_6=1.3237·10^7 cm^{-1} Å^6		A_{ex}=2.8609·10^4 cm^{-1} Å$^{-\gamma}$	
C_8=2.9889·10^8 cm^{-1} Å^8		γ=5.0081	
C_{10}=1.5821·10^{10} cm^{-1} Å^{10}		β=2.2085 Å^{-1}	
T_e^X=0 cm^{-1}		R_e^X=3.6434 Å	
D_e^X=5030.502(50) cm^{-1}		D_0^X=4977.187(50) cm^{-1}	

TABLE II. Pointwise representation of the potential energy curve for the $a\ ^3\Sigma^+$ state of NaRb.

R [Å]	U [cm^{-1}]	R [Å]	U [cm^{-1}]
2.944440	29489.89467	6.468399	4872.49275
3.155560	18461.93317	6.605337	4882.75826
3.366670	12363.70802	6.794944	4896.83178
3.577780	8991.52099	6.984550	4910.34530
3.788890	7126.77387	7.174157	4923.07187
4.000000	6095.47898	7.363764	4934.83385
4.198190	5552.35782	7.553371	4945.59408
4.396380	5237.10044	7.990520	4966.55716
4.594570	5062.99324	8.427668	4982.64596
4.792760	4957.08727	8.864817	4994.72299
4.990949	4890.76470	9.301966	5003.67683
5.189139	4852.15516	9.739114	5010.27403
5.387328	4832.98126	10.176263	5015.16200
5.585518	4827.17289	10.941010	5020.80312
5.783708	4830.40026	11.705758	5024.24404
5.920646	4836.15057	12.470505	5026.30776
6.057584	4843.78306	13.235253	5027.62932
6.194522	4852.68409	14.000000	5028.49121
6.331461	4862.36273		
U_∞=5030.50235 cm^{-1}			
R_o=11.3370 Å			
C_6=1.3237·10^7 cm^{-1} Å^6		A_{ex}=2.8609·10^4 cm^{-1} Å$^{-\gamma}$	
C_8=2.9889·10^8 cm^{-1} Å^8		γ=5.0081	
C_{10}=1.5821·10^{10} cm^{-1} Å^{10}		β=2.2085 Å^{-1}	
T_e^a=4827.14727 cm^{-1}		R_e^a=5.6003 Å	
D_e^a=203.355(50) cm^{-1}		D_0^a=193.365(50) cm^{-1}	

quencies forming about 3700 differences. The potentials from Tables I and II reproduce these differences with a standard deviation σ=0.0025 cm^{-1} and a dimensionless standard deviation of $\bar{\sigma}$=0.63, and they reproduce the total experimental data for the triplet state with σ=0.0035 cm^{-1} and $\bar{\sigma}$=0.59, and for the singlet state with σ=0.0032 cm^{-1} and $\bar{\sigma}$=0.73.

Figure 6 gives the magnitude of singlet-triplet coupling by the deviations of energy levels of the $a\ ^3\Sigma^+$ and the $X\ ^1\Sigma^+$ states calculated with the coupled channels code from the eigenvalues of the single channel potentials. The several points for each vibrational level correspond to different rotational quantum numbers $[7<J''(N'')<27]$ [29]. The top and bottom axis for v_a and v_X, respectively are scaled such that the values v_a, v_X of the closest levels form a vertical line. The larger deviations appear for higher J'' (N''). Note that the deviations for singlet state levels are larger than for the corresponding triplet state levels. Therefore, long range analysis based only on singlet transitions would introduce larger systematic distortions in the fitted potential curve for large internuclear distances than analysis based only on triplet transitions. This statement can be indirectly confirmed making single channel calculations with the potentials from Tables I and II showing that the $a\ ^3\Sigma^+$ state potential reproduces differences between levels with $v_a>7$ with a $\bar{\sigma}$=0.70 (the coupled calculations give $\bar{\sigma}$=0.62) while the $X\ ^1\Sigma^+$ state potential reproduces differences between levels with $v_X>68$ with a $\bar{\sigma}$=2.18 (the coupled calculations give $\bar{\sigma}$=0.52). So within the present experimental uncertainty the triplet state can still be considered as a single state, whereas a single channel treatment of the $X\ ^1\Sigma^+$ state will lead to an incorrect description of the long range potential.

The combined analysis on both ground state potentials has led to a revision of the dissociation energy of the $X\ ^1\Sigma^+$ state reported in Ref. [11]. The difference between the minimum of the $X\ ^1\Sigma^+$ state and the Na(3S)–Rb(5S) atomic asymptote (with respect to the center of gravity of the hyperfine structure) amounts to D_e^X=5030.502 cm^{-1} with an estimated uncertainty of ±0.05 cm^{-1} (the uncertainties of the fitted parameters are discussed in Sec. IV). This should be compared to

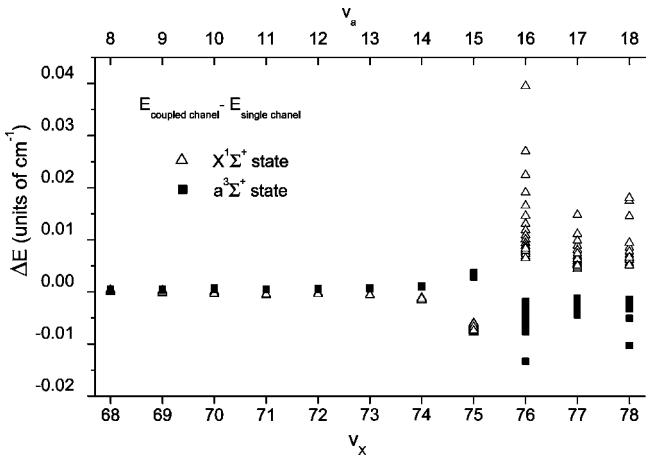

FIG. 6. Deviation ΔE of the energy level positions for the $a\ ^3\Sigma^+$ state (solid squares) and the $X\ ^1\Sigma^+$ state (open triangles) calculated with coupled channels code from the eigenvalues of the single channel potentials. Vibrational quantum numbers for the $a\ ^3\Sigma^+$ state, v_a are given on the top X axis whereas the vibrational quantum numbers for the $X\ ^1\Sigma^+$ state, v_X—on the bottom X axis. The several points for each vibrational level correspond to different rotational quantum numbers ($J''=N''=7-27$).

the 5030.848 cm^{-1} from Ref. [11] and the 5030.75 cm^{-1} from Ref. [33] in order to highlight the importance of the coupled channel analysis. The value of the dissociation energy with respect to the first rovibrational level amounts to $D_0^X=4977.187\ cm^{-1}$. The corresponding values for the triplet ground state are $D_e^a=203.355\ cm^{-1}$ and $D_0^a=193.365\ cm^{-1}$. The D_e^a differs significantly from the most recent value from Ref. [33] not only due to the improved experimental data set, but mainly due to the vibrational assignment established in this paper.

IV. DISCUSSION

A. Potential representation

Similar to the work on Ca_2 [36] parameters for the long range part of interatomic potentials were determined experimentally by fitting them to abundant and accurate experimental data. Contrary to the situation on the Ca_2 ground state asymptote [36], the structure of the pair of alkali metal Na and Rb atoms is much more difficult to model due to the presence of nonzero electronic and nuclear spins. Therefore, the direct estimation of the parameter uncertainties as done in Ref. [36] with Monte Carlo simulations would be very time consuming. Moreover, the experimental data in this study covers a narrower part of the long range potential than in the Ca_2 case. On the long range side the outermost classical turning point in NaRb at 15.6 Å has to be compared with 20 Å in the case of Ca_2. Due to the difference in the electronic structure of the Rb atom (open valence shell) and the Ca atom (closed subshell) the pure long range potential expression (2) cannot be extended to as small internuclear distances as for Ca_2. The narrower range not only increases the uncertainty of the fitted parameters, but also increases the ambiguity in connecting the long range potential to the pointwise representation (this problem was discussed in Ref. [36]). Also an additional degree of freedom was introduced in the fit—the term A_{ex} for the exchange energy expression (3) the correlation of which with C_6 was discussed in Ref. [36].

On the other hand a single set of long range parameters was fitted to data belonging to two different electronic states which gives desired constraint for the variation of the long range parameters. We want to point out that in the successive iterations the value U_∞ varied only between 5030.49 cm^{-1} and 5030.56 cm^{-1}, while the value of C_6 between $1.300\times10^7\ cm^{-1}$ Å^6 and $1.354\times10^7\ cm^{-1}$ Å^6. Although these intervals cannot be treated as some confidential limits, they still give some indication about the expected uncertainty of the fitted parameters.

The difficulty to provide the fitted long range parameters with a rigorous estimation of their uncertainty is not only because of the present experimental data set, but also because one of the main requirements—the smooth connection between the long range and the pointwise representation of the potentials—was not built into the fit. The problem here is not technical, but conceptual since in this case the uncertainty of the short range potential energy curve should be estimated which is delicate in the regions with a small amount of experimental data because the results become model dependent (see, e.g., [32,37,38]).

Therefore, we can state that the obtained potential curves are capable of describing the experimental data within actual error limits of 0.003 cm^{-1} and we prefer to postpone the discussion on the uncertainty of the fitted long range parameters until a reliable technique for its estimation is found.

It is worth mentioning that in the present analysis a direct experimental estimation of the exchange energy parameter A_{ex} was done. Since the other parameters (i.e., β and γ) were fixed to their estimated values from Ref. [18] and were not fitted we would avoid commenting directly on the physical meaning of A_{ex} alone. We would rather state that all three parameters together give a good representation of the exchange energy contribution, derived from a direct fit to experimental data.

Without being able to associate reliable uncertainty limits to the experimental dispersive coefficients and taking into account the strong correlation between them we cannot compare strictly our values with the recent *ab initio* predictions [16,17], although they are close to each other. In order to check the consistency of the theoretical calculations we tried to construct potential curves using values for C_6 and C_8 from [16,17] and fitting only C_{10} and A_{ex} to the experimental data prepared for the potential fit in Sec. III. The new potentials reproduce the experimental observations with similar quality which confirms the reliability of the theoretical coefficients. The analytic representations of these curves (definition in Ref. [35]) are given in Table III of the supplementary material [39].

B. Application to ultracold collisions

Because the present analysis includes the hyperfine structure of levels close to the atomic asymptote and does show

TABLE III. Scattering length (in a_0) of different isotopomers of NaRb.

	Triplet		Singlet	
Isotope	This work	Ref. [19]	This work	Ref. [19]
^{23}Na ^{87}Rb	70	96+18/−12	109	104+6/−6
^{23}Na ^{85}Rb	81	112+24/−18	396	315+100/−60

the reliability of the atomic parameters for such levels, it is justified to extrapolate shortly above the asymptote, thus in the regime of ultracold collisions. Experiments with a mixed species Magneto-Optical Traps (MOT) are expected from existing results of similar systems ([1,4,5]) and comparison with other theoretical estimations [18,19,21] is desired, especially with the predictions of Feshbach resonances in NaRb [20].

Weiss *et al.* [18] discussed the case of two-species Bose-Einstein Condensate (BEC) (TBEC) for Na and Rb, because both types of ultracold ensembles could be condensed and also the ^{85}Rb ensemble was successfully condensed by magnetic tuning the scattering lengths. In Ref. [18] the authors used for the calculation of scattering length the singlet ($X\,^1\Sigma^+$) and triplet ($a\,^3\Sigma^+$) potentials which they constructed from experimentally determined curves from Refs. [22,33] and theoretical results for the long range parameters [16]. Because their calculation gave only a very small difference between the triplet and singlet scattering lengths for the isotopomer ^{23}Na^{87}Rb they concluded that spin exchange collisions will play a minor role and the elastic scattering lengths for the different hyperfine pairs of collisions will be nearly equal.

With our results we almost closed the gap of asymptotic levels to the atomic asymptote. Additionally, recent theoretical results appeared [17]. In our present analysis we have revised the vibrational assignment of the $a\,^3\Sigma^+$ state and thus its potential depth is larger than in the work by Weiss *et al.* [18]. Therefore, the scattering properties for the triplet case and consequently for the hyperfine cases might be significantly different to the predictions in Refs. [18,20].

We give our results in Table III, from which one can see, that the difference between singlet and triplet scattering length for ^{23}Na ^{87}Rb now becomes $39a_0$ (a_0=0.529 18 Å) instead of $8a_0$ by Weiss *et al.* [19], which results in significant larger spin-exchange probabilities in Na-Rb collisions determined by the difference of both scattering lengths. Error estimations are similar to those presented by Weiss *et al.* [18], because they are mainly related to reliability of the long range parameters, where our own derivations confirm the theoretical results but could not reduce the error limits. We do not include in the present comparison the calculations by Ouerdane *et al.* [21], because they obviously overlooked the erratum [19] from Weiss *et al.* Thus numbers from Ref. [21] might lead to confusion.

For future studies on ultracold ensembles of Na and Rb, their miscibility, their sympathetic cooling behavior, inelastic cross sections for the discussion of trap loss, etc., are of great importance. Thus we searched for Feshbach resonances for

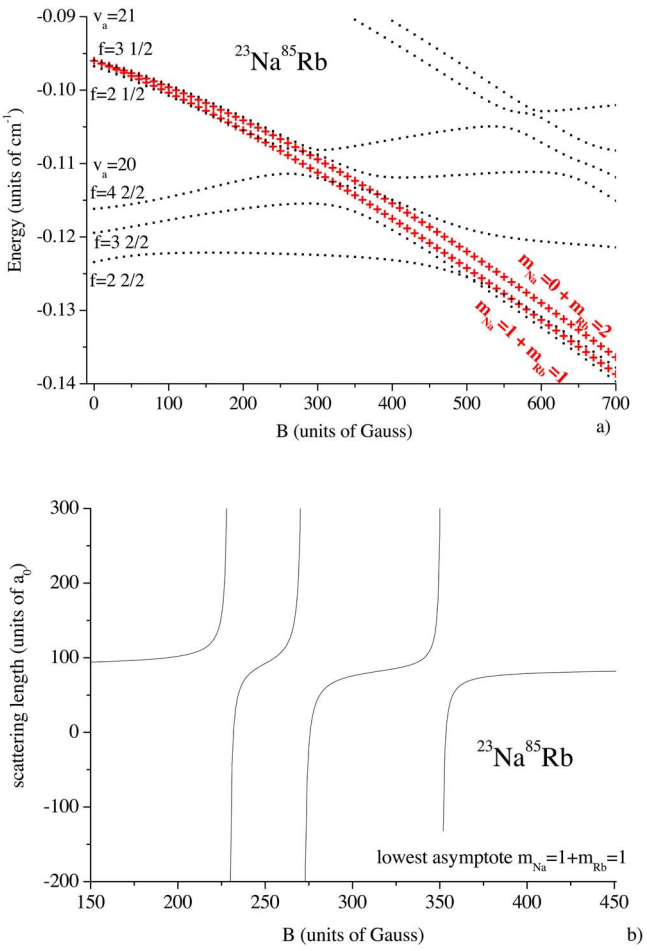

FIG. 7. (Color online) (a) Energy levels of the $a\,^3\Sigma^+$ and $X\,^1\Sigma^+$ coupled system as function of magnetic field for Zeeman component $M=2$. The reference of the energy scale is at U_∞ (for details see the text). (b) Scattering length for the lowest $m_{Na}=1+m_{Rb}=1$ asymptote as a function of magnetic field. Below 250 G no resonances appear.

different Zeeman sublevels in ^{23}Na ^{87}Rb and ^{23}Na^{85}Rb and found in many cases resonances below 500 Gauss, which will be easily accessible in an experiment in which the cold ensemble is transferred from a traditional MOT to an optical dipole trap. We calculated the full hyperfine structure to identify the quantum states responsible for these resonances, which are indicated in Fig. 7(a). The crosses follow the two low asymptotes with $M=2$ and squares give the bound or quasibound levels. One sees immediately the 3 bound states, crossing the asymptote, which are responsible for the three resonances shown in Fig. 7(b), where the s wave scattering length as a function of magnetic field for the lowest Zeeman level with $M=2$, ^{23}Na$(f,m=1,1)+^{85}$Rb$(f,m=2,1)$ is calculated. Quantum numbers are given on the left side, where f stands for the total angular momentum (s wave, $l=0$) and the two numbers separated by a slash for the asymptotic atomic angular momenta. We confirmed, by calculating the collision resonances above the asymptote, that these resonances stay quite narrow in an energy range up to 1 mK, namely about 100 kHz, which means that corresponding quasibound states

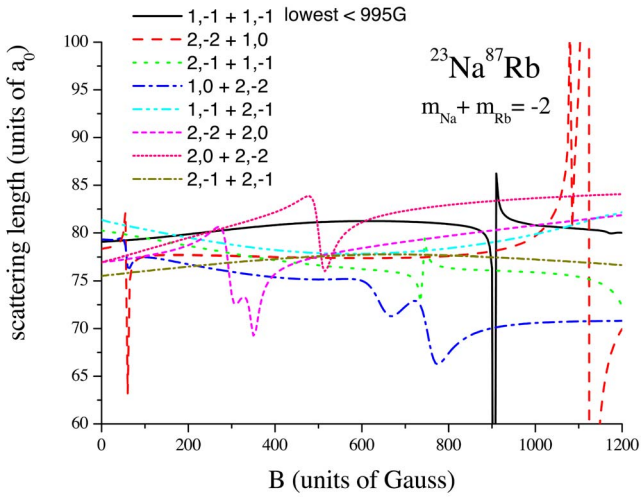

FIG. 8. (Color online) Scattering length as a function of magnetic field for Zeeman component $M=-2$ and the different collision asymptotes indicated by label $f_{Na},m+f_{Rb},m$ for ^{23}Na ^{87}Rb.

have lifetimes in the range of 10 μs and can play a significant role as intermediate steps in producing ultracold molecules. The states are strongly mixed singlet-triplet levels, where the vibrational levels 80 and 21 of the singlet and triplet state are mainly involved, respectively; in Fig. 7 only the vibrational quantum number of the triplet state is indicated.

For the same isotopomer the collision of the magnetically trappable pair $\mathrm{Na}(f,m=1,-1)+\mathrm{Rb}(f,m=2,-2)$ was calculated, because for Rb this Zeeman level was applied for BEC and we found Feshbach resonances around 170 and 430 G which originate from quasibound levels ($f=3$ and 4 with atomic asymptote 1+3) coming from above the considered collision asymptote thus leading to a negative scattering length at low magnetic fields and positive on the other side of the resonance.

Bhattacharya *et al.* [20] presented estimations of Feshbach resonances for ^{23}Na^{87}Rb at several asymptotes for $M=-2$: $\mathrm{Na}(f,m=1,-1)+\mathrm{Rb}(f,m=2,-1)$, $\mathrm{Na}(f,m=1,0)+\mathrm{Rb}(f,m=2,-2)$, and $\mathrm{Na}(f,m=2,-1)+\mathrm{Rb}(f,m=2,-1)$ using the same potential construction as in Ref. [18] and including the hyperfine structure and the Zeeman energy by diagonalizing the potential matrix and applying the obtained adiabatic potentials for determining the bound state levels which cross the collision asymptotes. In Fig. 8 we present our results (strictly speaking the real part of the scattering length) from closed coupling calculations on these asymptotes in the magnetic field range up to 1200 G in steps of 5 G. In each case except the highest one we obtain Feshbach resonances of very different widths, because of the finite step size (5 G) in the calculation the curves are not going to infinity for sharp resonances where inelastic contributions do not lead to a complex valued scattering lengths. For the asymptote $\mathrm{Na}(f,m=1,0)+\mathrm{Rb}(f,m=2,-2)$ we find two very broad resonances (635 and 750 G) which are close to values given in Ref. [20] but for the other cases we find resonances at very different values or none up to 3000 G. This result is not surprising because the triplet potential was obtained by a revised assignment and now contains 23 vibrational levels instead of 22 from Ref. [18]. Also the singlet potential was derived from experimental data much closer to the dissociation asymptote than earlier (the number of vibrational levels in the singlet state potential well remains 83 as in Ref. [11]). From simple estimations using the different potential approaches during our fitting process we believe that the resonances are described with an uncertainty of ±50 G, which will be helpful for planning experiments.

In concluding, we note that we could derive a highly reliable potential scheme which already allows us to describe ultracold collisions including hyperfine interaction and the Zeeman effect. We found low magnetic fields for a large number of Feshbach resonances and this fact might be attractive to study the collision dynamics in these mixed ultracold ensembles, the conditions of miscibility can be altered and the realization of two-species BEC in NaRb might be achievable. Any direct observation of Feshbach resonances can be incorporated in the present potential fit to improve the prediction power of the model. We are planning experiments in which a molecular beam and pump-probe schemes are applied for reaching the closest levels at the asymptotes as it was done in Na_2 [36] for example. Such results will also lead to fix the asymptotic phase shifts of a collision and thus the scattering lengths.

ACKNOWLEDGMENTS

The work is supported by DFG through SFB 407 and GRK 665. O.D., M.T., and R.F. acknowledge the support by the NATO SfP 978029 Optical Field Mapping Grant and by the EC 5th Frame "Competitive and Sustainable Growth" Grant No. G1MA-CT-2002-04063, as well as by the Latvian Science Council Grant No. 04.1308 and Latvian Government Grant No. TOP 04-44. A.P. acknowledges the support from the Alexander von Humboldt Foundation.

[1] Z. Hadzibabic, C. A. Stan, K. Dieckmann, S. Gupta, M. W. Zwierlein, A. Görlitz, and W. Ketterle, Phys. Rev. Lett. **88**, 160401 (2002).

[2] G. D. Telles, L. S. Aguiar, L. G. Marcassa, and V. S. Bagnato, Phys. Rev. A **66**, 025403 (2002).

[3] C. Haimberger, J. Kleinert, M. Bhattacharya, and N. P. Bigelow, Phys. Rev. A **70**, 021402(R) (2004).

[4] J. P. Shaffer, W. Chalupczak, and N. P. Bigelow, Phys. Rev. A **60**, R3365 (1999).

[5] G. Ferrari, M. Inguscio, W. Jastrzebski, G. Modugno, G. Roati, and A. Simoni, Phys. Rev. Lett. **89**, 053202 (2002).

[6] D. Wang, J. Qi, M. F. Stone, O. Nikolayeva, H. Wang, B. Hattaway, S. D. Gensemer, P. L. Gould, E. E. Eyler, and W. C. Stwalley, Phys. Rev. Lett. **93**, 243005 (2004).

[7] S. Inouye, J. Goldwin, M. L. Olsen, C. Ticknor, J. L. Bohn, and D. S. Jin, Phys. Rev. Lett. **93**, 183201 (2004).
[8] A. J. Kerman, J. M. Sage, S. Sainis, T. Bergeman, and D. DeMille, Phys. Rev. Lett. **92**, 153001 (2004).
[9] S. Kasahara, T. Ebi, M. Tanimura, H. Ikoma, K. Matsubara, M. Baba, and H. Katô, J. Chem. Phys. **105**, 1341 (1996).
[10] M. Tamanis, R. Ferber, A. Zaitsevskii, E. A. Pazyuk, A. V. Stolyarov, H. Chen, J. Qi, H. Wang, and W. C. Stwalley, J. Chem. Phys. **117**, 7980 (2002).
[11] O. Docenko, M. Tamanis, R. Ferber, A. Pashov, H. Knöckel, and E. Tiemann, Phys. Rev. A **69**, 042503 (2004).
[12] P. Kortyka, W. Jastrzebski, and P. Kowalczyk, Chem. Phys. Lett. **404**, 323 (2005).
[13] W. Jastrzebski, P. Kortyka, P. Kowalczyk, O. Docenko, M. Tamanis, R. Ferber, A. Pashov, H. Knöckel, and E. Tiemann, Eur. Phys. J. D **36**, 57 (2005).
[14] O. Docenko, M. Tamanis, R. Ferber, A. Pashov, H. Knöckel, and E. Tiemann, Eur. Phys. J. D **49**, 57 (2005).
[15] M. Marinescu and H. R. Sadeghpour, Phys. Rev. A **59**, 390 (1999).
[16] A. Dervianko, J. F. Babb, and A. Dalgarno, Phys. Rev. A **63**, 052704 (2001).
[17] S. G. Porsev and A. Derevianko, J. Chem. Phys. **119**, 844 (2003).
[18] S. B. Weiss, M. Bhattacharya, and N. P. Bigelow, Phys. Rev. A **68**, 042708 (2003).
[19] S. B. Weiss, M. Bhattacharya, and N. P. Bigelow, Phys. Rev. A **69**, 049903(E) (2004).
[20] M. Bhattacharya, L. O. Baksmaty, S. B. Weiss, and N. P. Bigelow, Eur. Phys. J. D **31**, 301 (2004).
[21] H. Ouerdane and M. J. Jamieson, Phys. Rev. A **70**, 022712 (2004).
[22] O. Docenko, O. Nikolayeva, M. Tamanis, R. Ferber, E. A. Pazyuk, and A. V. Stolyarov, Phys. Rev. A **66**, 052508 (2002).
[23] Y.-C. Wang, M. Kajitani, S. Kasahara, M. Baba, K. Isikawa, and H. Katô, J. Chem. Phys. **95**, 6229 (1991).
[24] Y.-C. Wang, K. Matsubara, and H. Katô, J. Chem. Phys. **97**, 811 (1992).
[25] W. Jastrzebski, P. Kortyka, P. Kowalczyk, and A. Pashov (unpublished).
[26] W. Jastrzebski, P. Kowalczyk, and A. Pashov, J. Mol. Spectrosc. **209**, 50 (2001).
[27] Ch. Lisdat, O. Dulieu, H. Knöckel, and E. Tiemann, Eur. Phys. J. D **17**, 319 (2002).
[28] H. Knöckel, B. Bodermann, and E. Tiemann, Eur. Phys. J. D **28**, 199 (2004).
[29] The symbol N is used for the Hund's case (b) triplet state because the total angular momentum J is the sum of N and spin S.
[30] A. A. Radzig and P. M. Smirnov, *Reference Data on Atoms, Molecules and Ions* (Springer, Berlin, 1985).
[31] A. Pashov, W. Jastrzębski, and P. Kowalczyk, Comput. Phys. Commun. **128**, 622 (2000).
[32] A. Grochola, W. Jastrzebski, P. Kowalczyk, and A. Pashov, J. Chem. Phys. **121**, 5754 (2004).
[33] W. T. Zemke and W. C. Stwalley, J. Chem. Phys. **114**, 10811 (2001).
[34] F. H. Mies, E. Tiesinga, and P. S. Julienne, Phys. Rev. A **61**, 022721 (2000).
[35] C. Samuelis, E. Tiesinga, T. Laue, M. Elbs, H. Knöckel, and E. Tiemann, Phys. Rev. A **63**, 012710 (2000).
[36] O. Allard, C. Samuelis, A. Pashov, H. Knöckel, and E. Tiemann, Eur. Phys. J. D **26**, 155 (2003).
[37] W. Jastrzebski, P. Kowalczyk, and A. Pashov, J. Chem. Phys. **114**, 10725 (2001).
[38] O. Allard, A. Pashov, H. Knöckel, and E. Tiemann, Phys. Rev. A **66**, 042503 (2002).
[39] See EPAPS Document No. PLRAAN-72-109512 for (brief description). This document can be reached via a direct link in the online article's HTML reference section or via the EPAPS homepage (http://www.aip.org/pubservs/epaps.html).